HYBRID CARBON BASED CONDUCTING POLYMER NANOCOMPOSITE FOR IMPROVED ELECTROMAGNETIC INTERFERENCE SHIELDING EFFECTIVENESS

Abstract

The growing demand for high-quality electronic and communication devices in military, industrial, and commercial applications has resulted in electronic device and system compactness, which increases circuit complexity. This is a novel form of challenge that necessitates a slew of decisions on electromagnetic radiation as a result of repeated efforts. These electromagnetic radiations interfere with one another and have the potential to ruin the system, which is referred to as electromagnetic (EM) pollution. Because it interferes with the operation of a device or transmission channel, electromagnetic interference is a key source of concern. To solve this issue, scientific and research organizations have started to create a variety of materials for electromagnetic interference (EMI) shielding applications. Carbon has long been an enthralling chemical; allotropes of carbon, such as fullerenes, graphite, graphene, carbon nanotubes, and other fillers that improve EMI shielding, are of significant interest in a variety of frequency bands. Initially, Multiwalled Carbon Nanotubes (MWCNT) and Graphene (GNS) were functionalized to improve conducting polymer interface. Polyaniline/Carbon nanotube/Graphene (PANI)/(MWCNT)/(GNS) were synthesized using an in situ oxidative polymerization process, with the weight percent of MWCNT remaining constant while the weight percent of GNS increasing from 1-3, and then characterized using SEM and FTIR analysis. When compared to pure polyaniline, the electrical conductivity of the nanocomposites rises with increasing weight percent of GNS. Carbon-based conducting polymer nanocomposites demonstrated semi

Authors

P.R.Modak
Department of Physics
RMGACS College
Saoli, Maharashtra, India.

D.V.Nandanwar
Department of Physics
M.M. Science College
Nagpur, Maharashtra, India.

conductivity and improved EMI shielding performance. The EMI Shielding effectiveness (SE) of hybrid carbon-based conducting polymer nanocomposites grows as the weight percent of GNS increases. Absorption is the major mechanism for synthesized ternary nanocomposites and can be employed as an Electromagnetic Interference shielding material.

Keywords: Electromagnetic Interference Shielding; Ternary Nanocomposites; Conducting Polymers

I. INTROUCTION

Because of the rapid rise of nanoscience and nanotechnology, the electronic industries have thrived. The electronic system within the instrument is tiny and densely packed with electrical components. This massive growth in electrical, telecommunications, and instrumentation results in an unwelcome and unfavorable consequence known as electromagnetic interference (EMI). A signal that is conducted and/or transmitted is referred to as electromagnetic interference (EMI). It is produced by any equipment or apparatus that transmits, distributes, processes, or uses electrical energy in any way. This EMI may interact with any other electronic device in the same area, reducing the performance of other equipment or systems. Receiving equipment can be affected by EMI, leading it to malfunction or fail. The effects of electromagnetic interference are becoming more visible as a result of increased demand for high-speed electronic devices operating at extremely high frequencies, the more demanding use of electronics in computers, communication equipment such as mobile and smart phones operating at 2-3 GHz for data transmission, and the miniaturization of these electronic devices. Electronic noise grows when electronic components become more compact and tightly packed. EMI may also have an impact on space exploration, military machinery, electronic devices, and communication instruments, among other things [1]. On a daily basis, people work and live in a state of electromagnetic radiation. Electromagnetic radiation not only impairs normal equipment operation, but it also has an effect on the human body [2]. As a result, EMI radiation blocking methods must be provided to isolate an appliance's microscopic electrical components from the surrounding environment. To manage the amount of electromagnetic (EM) energy created by the circuit that can escape into the external environment or to limit the amount of EMI radiation from the external environment that can penetrate the circuit, a shielding material must be provided. The blocking of electromagnetic radiation by a barrier made of conductive or magnetic material is known as electromagnetic interference shielding. The shield must completely wrap the device and contain no penetrations such as holes, slots, or cables in order to function. Any hole in a shield can greatly reduce its effectiveness. The main reason for good shield design is to construct a device that meets National/International Electromagnetic Interference Regulatory Standards [3]. Excessive use of electronic devices such as cell phones, laptop computers, and others can result in a range of ailments including leukemia, breast cancer, migraines, heart attacks, and even miscarriages. As a result, electromagnetic radiation pollutes the environment and poses a health risk to humans. It also has a deleterious impact on electronic gadgets [4]. Polymers are organic substances with a high molecular weight. A polymer is composed of several small molecules known as monomers. A monomer is a substance with a low molecular weight that, when mixed with other substances, generates a polymer with a high molecular weight [5]. Traditional polymers, such as plastic rubber, are dielectrics or insulators due to their great resistance to electric conduction. In the mid-1970s, conducting polymers were created. Scientists Hideki Shirakawa, Alan MacDiarmid, and Alan Heeger announced the discovery of polyacetylene doped with halogens, the simplest conducting polymer. The term "synthetic metals" refers to a new class of conducting polymers [6,9]. Conducting polymers are metal-like compounds with semiconductor characteristics. Conjugated double bonds along the polymer backbone are an important property of conductive polymers. [6]. Most polymeric materials are poor conductors of electricity because a large number of free electrons are not available to participate in the conduction process [5]. Doping significantly boosts the electrical conductivity of conducting polymers [10]. Andre Geim and colleagues at the University of Manchester discovered

graphene using the seemingly simple Scotch tape method, igniting a revolution in Condensed Matter Physics. The 2004 discovery by Geim and Novoselov et al. of a method for generating individual graphene sheets ignited a frenzy of scientific activity [11]. The Nobel Prize in Physics was awarded to Andre Geim and Konstantin Novoselov in 2010 for their "groundbreaking experiments on the two-dimensional material graphene." The two researchers revealed that carbon in such a flat form contains exceptional quantum physics-derived properties. Graphene is not only the thinnest substance known, but it is also 200 times stronger than steel and conducts electricity better than any other material known to man at room temperature. Graphene, according to Columbia University researchers, is the strongest substance ever measured. Since then, graphene has been marketed as the next-generation material for nano-electronic devices [12].

Graphene is a graphite derivative [13]. A conductive nanomaterial is a one-atom-thick planar sheet of sp2 connected carbon atoms [14-16]. It is a two-dimensional hexagonal lattice. Figure 1.1 depicts the honeycomb structure of the sheet [17, 18].

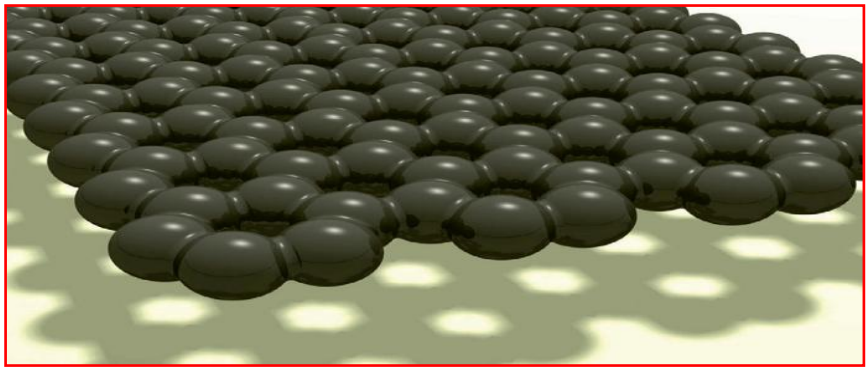

Figure 1.1: Structure of Graphene

Graphene is recognized as the critical underpinning for fullerene allotropic dimensionalities. In addition to its planar state, graphene may be 'wrapped' into zero-dimensional spherical buckyballs or C60 and 'rolled' into one-dimensional Carbon Nanotubes (CNTs) [18, 19]. Carbon nanotubes were further categorized as single-walled or multi-walled (SWCNTs/MWCNTs) depending on the number of graphene layers present [14]. Graphite is a three-dimensional stack of graphene layers held together by van der Waals forces [20-22]. In other words, as a building block, graphene is the "mother of all carbon forms" [14]. When infinite graphene crystals become limited, surface and boundaries emerge, generating non-three coordinated atoms with nanoscale dimensions at the edges. The graphitic nanostructure's characteristics differ from those observed in bulk. Graphitic nanostructures include nanoribbons and nanoclustures [23]. Carbon atoms in graphene form a strong lattice and a p- orbital perpendicular to the graphene plane, resulting in a delocalized p electron system. At low energies, the linear energy dispersion relation associated with massless electrons, or Dirac fermions, results in a material with a zero band gap and a linear density of states [24]. Graphene offers a variety of intriguing features. It is impermeable to gases. Individual graphene has also been found to have improved electronic transport properties [25]. Graphene is a rising star in the world of nanomaterials due to its exciting properties, which include sensors, transistors, terahertz imaging, composites, energy storage devices, batteries, and thin coatings for solar cells, LCD displays, and electromagnetic interference

shielding [23]. Iijima developed carbon nanotubes (CNTs), which have subsequently helped to enhance research in the disciplines of physics, chemistry, and material sciences. Many works have been conducted on the structure, properties, and prospective uses. Because of their cylindrical geometry and nanometric scale, carbon nanotubes are excellent for potential uses such as hydrogen storage. Because of their well-defined atomic structure, high length to diameter ratio, and chemical stability, single wall carbon nanotubes (SWNTs) is one-dimension molecules. SWNTs have specific electrical properties and can be metallic or semiconducting depending on their geometry [26]. Carbon nanotubes are sheets of graphite that have been coiled into tubes. Nanotubes are regarded to be almost one-dimensional structures due to their remarkable length to diameter ratio. The most important structures are depicted in Figure 1.2, which are single walled nanotubes (SWNTs) and multi walled nanotubes (MWNTs). A SWNT is a cylinder that contains only one wrapped graphene sheet. MWNTs are multiwalled nanotubes that resemble a ring of concentric SWNTs. The length and diameter of these structures, as well as their properties, differ greatly from those of SWNTs [27].

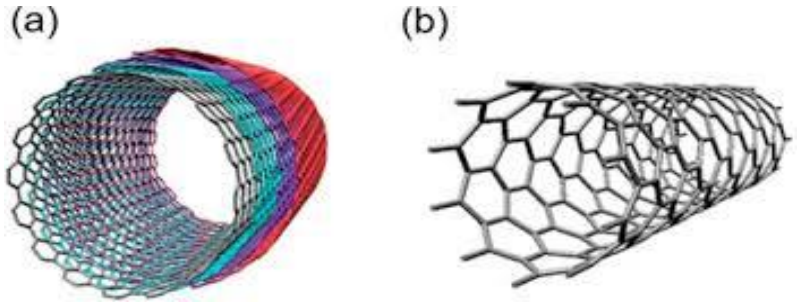

Figure 1.2: (a) Multi walled nanotubes (MWNTs), (b) Single walled nanotubes (SWNTs)

The most common methods for manufacturing SWNTs and MWNTs are carbon-arc discharge, laser ablation of carbon, or chemical vapour deposition (typically on catalytic particles). The most prevalent method of generating high-volume CNTs is chemical vapour deposition (CVD), which uses fluidized bed reactors that allow consistent gas flow and heat transmission to metal catalyst nanoparticles. The diameters of SWNT nanotubes range from 0.4 to 3 nm, while MWNT diameters range from 1.4 to at least 100 nm. A nanotube's diameter can thus be exploited to alter its properties. Unfortunately, SWNTs are currently only produced on a small scale and at a high cost. The exceptional mechanical, electrical, transport, vibrational, thermal, and other properties of carbon nanotubes, most of which are due to their quasi-one-dimensional sp2-bonded structure [28,29]. Carbon nanotubes have grabbed the interest of many scientists worldwide. Because of their small size, strength, and extraordinary physical properties, these structures are a very uncommon material with a wide range of intriguing applications. They can be used as mechanical reinforcements in high performance composites, as nanotube-based field emitters, as nanoprobes in metrology and biological and chemical investigations, and as templates for the creation of other nanostructures. The electronic properties of carbon nanotubes allowed them to be used in device applications. They have a wide range of applications in energy storage, sensors, supercapacitors, and other domains [30] . Polymer nanocomposites (PNC) are polymers that have been reinforced in small amounts (less than 5% by weight) with nano-sized particles with high aspect ratios (L/h >300). To create polymer nanocomposites reinforced with filler

nanoparticles, four interdependent areas must be balanced: constituent selection, cost-effective processing, fabrication, and performance. The matrix, reinforcement (fibre), and interfacial region are the three major material elements of any composite. The interfacial area is responsible for communication between the matrix and the filler due to its proximity to the filler's surface, and its properties differ from those of the bulk matrix. The nanoparticles introduced to the matrix or matrix precursors are made up of two types of nanoparticles based on this grouping: (i) low-dimensional crystallites and (ii) aggregates [31]. In recent years, the dispersion of nanoparticles CNT/GNS in a polymer matrix has emerged as a fresh and fascinating topic in materials research. Traditional composites and pure polymers cannot compete with the qualities of these nanocomposite materials. The increased properties are due to the dispersion of the nanofillers in the polymer matrix. Even at low filler loadings in the polymer matrix, the properties of these nanocomposites improve [32]. Because these nanocomposites have a positive temperature co-efficient, resistance increases as temperature rises. [33].

1. **Literature Review:** Metals were previously used as EMI shielding materials in the form of thin sheets or sheathing; however, metals were costly, heavy, prone to corrosion, and difficult to manufacture. As a result, conducting polymers and composites with conductive fillers were developed as an alternative EMI shielding material. These materials are lightweight, low-cost, corrosion-resistant, and easy to work with. Because of their vast range of uses, conducting polymers (CPs) have gained importance in the last four decades. Carbon nanofibres, carbon nanotubes, and graphene are gaining prominence because to their high aspect ratio and potential applications as ideal absorbers.

   Chen and colleagues Sai Hu et al prepared the PANI/CuS/reduced graphene oxide (RGO) composites, which exhibit remarkably enhanced shielding effectiveness. The average EMI SE of composites with a thickness of 3mm reached -18dB from -7.5dB in the frequency range of 300 KHz-3GHz. Wu et al created a combination of graphene foam (GF) and poly(3,4-ethylenedioxythiophene):poly(styrenesulfonate) (PEDOT:PSS). The GF/PEDOT:PSS composites had an ultralow density of 18.2X10-3 g/cm3 and a high porosity of 98.8%, as well as a nearly fourfold increase in electrical conductivity from 11.8 to 43.2 S/cm after the introduction of the conductive PEDOT:PSS. The composites exhibit extraordinary EMI shielding performance with a shielding efficiency (SE) of 91.9 dB thanks to their superior electrical conductivity, extremely light porous structure, and effective charge delocalization. Cheng et al synthesized a high heat- resistance crystallite, stereo complex crystallites (Sc), by stereocomplexation crystallization of enantiomeric poly(L-lactide) (PLLA) and poly(D-lactide) (PDLA), and introduced it into a conductive carbon nanotube (CNT)/ Poly(lactic acid) (PLA) composite foam. The freeze-dried CNT/ PLA foam has a low foam density of 0.10 g/cm^3 and a high 216 dB cm^3/g specific EMI shielding efficacy. Jeddi et al developed hybrid polyurethane foam/silicon rubber/carbon black/nanographite composites, and the EMI SE results showed that reflection loss was the primary shielding mechanism in all samples. Fletcher et al. developed an elastomer nanocomposite of MWCNTs in a fluorocarbon polymer, with EMI SEs of 50 dB for a MWCNT filler loading of 12 wt% and 20 dB for a loading of 6 wt%. Their measured samples, on the other hand, were relatively thick (3.8 mm). To lower the size and weight of electronic gadgets, the EMI shielding materials that surround them should be thin as well. They reported that the EMI SE for MWCNT filler loading of 12 wt% was around 15 dB when the thickness was 0.8 mm, because the EMI SE in decibels is roughly

proportional to thickness. Keto et al created a flexible and elastic EMI shielding material by incorporating SG-CNTs (1 wt%) into a fluorinated rubber, resulting in a high EMI SE (20 dB, 90% shielding) without hardening or embrittling the rubber. Choudhary et al created flexible shielding materials comprised of Fe_3O_4 nanoparticles, mesocarbon microbeads, and multiwalled carbon nanotubes (MCMBs/MWCNTs) composite paper for excellent EMI shielding in the X-band. The addition of Fe_3O_4 nanoparticles in the MCMBs/MWCNTs composite paper improves its interfacial polarisation and anisotropy energy, resulting in an outstanding absorption dominated EMI shielding effectiveness (SE) of 80 dB at 0.5 mm thickness. Sing et al. and colleagues created a three-dimensional (3D) nanostructure comprised of chemically modified graphene/Fe_3O_4(GF) integrated polyaniline as a high-performance shielding material against electromagnetic pollution. Verma et al created a ternary hybrid nanocomposite with a thermoplastic polyurethane matrix and a filled inclusion of graphene nanoplates carbon nanotubes hybrid (GCNT). For a 10% loaded GCNT sample, these hybrid nanocomposites demonstrated good electromagnetic interference shielding of up to 47 dB in the Ku-band of microwave frequency. Rao et al developed lightweight, flexible, and thin Fe_3O_4-loaded, functionalized multiwalled carbon nanotube buck papers for enhanced X-band electromagnetic interference shielding. A buck paper with a thickness of 50 m and a density of 0.51 g cm^{-3} exhibits a high total specific shielding effectiveness of around 49.56 dB.

II. MATRIALS AND METHODS

1. **Materials:** Merck Limited., India supplied the chemicals, which included aniline ($C_6H_5NH_2$), sulphuric acid (H_2SO_4), nitric acid (HNO_3), and ammonium persulfate [$(NH_4)_2S_2O_8$]. Graphite flakes and carbon nanotubes (CNTs) are now available from NPL in New Delhi, India. Aniline was distillated under reduced pressure and at temperatures below 4 degrees Celsius. Distilled water was employed in all synthesis processes.

2. **Synthesis of Polyaniline (PANI):** Before usage, aliline was distilled and stored at temperatures below 5^oC. Polyaniline was created by the chemical oxidative polymerization technique. The 0.2M H_2SO_4 solution in 50 ml of deionized water was divided in half. The mixture was agitated for roughly 5 hours after one part 0.2M aniline was added. Another half was mixed with 0.2M ammonium persulphate (APS) and added to the whirling monomer solution drop by drop. After mixing the reactants, the solution turns greenish before turning violet. The dark precipitate was recovered after 6 to 7 hours. This hue indicates that the product was in the conducting phase of emerald salt. This precipitate was allowed to settle overnight before being diluted with deionized water until the filter was colorless. Finally, it was cleaned with ethanol and dried overnight in an oven at 80^oC [34-36].

3. **Synthesis of Graphite Oxide (GO) and Graphene Nanosheets (GNS):** The Hummers method was used to synthesize graphite oxide (GO) from graphite flakes, and GO exfoliation was used to produce graphene nanosheets (GN). A typical process was combining the appropriate amount of graphite flakes and $NaNO_3$ with H2SO4. Potassium permanganate was gently added to the suspension while rapidly swirling for 1 hour at low temperature. The reaction system was stirred at room temperature to generate a thick paste. As the reaction progressed, the mixture became pasty and the colour changed to a

light brownish hue. Finally, with vigorous agitation, H_2O_2 was gradually added to the pasty, altering its hue from brown to yellow. After that, the GO was vacuum filtered and washed with deionized water. Exfoliation was achieved by sonicating the GO dispersion for 30 minutes at room temperature. To create graphene nanosheets, ammonia solution and hydrazine monohydrate were added to a sonicated GO dispersion, and the mixture was heated at 90^oC for 2 hours with vigorous stirring. Following the completion of the process, the reduced graphene nanosheets (GNS) were collected as a black powder by filtration [37-45].

4. **Functionalization of Graphene and Carbon Nanotubes:** Functionalized graphene (FGNS) or functionalized carbon nanotubes (CNT) are graphene or CNT that have been changed by adding additional functional groups to their surfaces. By modifying the surface of to obtain functional groups that act as precursors for the anchoring of suitable organic/inorganic molecules, as well as to improve its dispersion in solvents, functionalization improves the properties. This serves as a substrate for nanoparticle nucleation and growth, resulting in homogeneous size distribution and nanoparticle deposition on two-dimensional nanosheets. There are two types of functionalization approaches for grapheme and carbon nanotubes: covalent and noncovalent techniques. Covalent and noncovalent modification approaches are both extremely effective in producing process able graphene [46,47].

   The surface functional groups of graphene nanosheets are constrained, allowing for chemical interactions with polymers. As a result, acid treatment was used to functionalize GNS. A solution of 6M H_2SO_4 and 6M HNO_3 in a 3:1 ratio was agitated for 10 minutes to functionalize GNS. GNS was added to the solution, which was then sonicated for 4 hours at 50oC. GNS was centrifuged and then filtered, washed, and dried to produce functionalized GNS [48, 49]. The same process was used to functionalize carbon nanotubes.

5. **Synthesis of PANI/CNT/GNS Composites:** An in-situ chemical oxidative polymerization of aniline in the presence of CNT/GNS was used to create the PANI/CNT/GNS composites. The weight percentage of CNT remained constant while the weight percentage of GNS to aniline fluctuated from 0% to 5%. The 0.2M H2SO4 solution in 50 ml of deionized water was separated into two halves. The mixture was ultrasonicated for 30 minutes after adding 0.2M aniline and functionalized CNT/GNS to one portion. After ultrasonication, the mixture was stirred for around 5 hours at 5oC to maximize yield. Another half was combined with 0.2M ammonium persulphate (APS) and added drop by drop to the swirling monomer solution. After combining the reactants, the solution takes on a greenish color before turning violet. After 6 to 7 hours, the black precipitate was collected. This precipitate was left overnight before being diluted with deionized water until the filtrate was colorless. Finally, it was rinsed with ethanol and dried in an oven at 80oC [50-57] overnight.

III. RESULT

1. **Scanning Electron Microscopy:** Nanocomposites under research must be characterized in order to understand the structure, morphology, and interaction of different components. SEM can be used to study the morphological and structural aspects of composites [56].

This study used scanning electron microscopy (SEM) to provide surface information on the materials as well as a complete assessment of the morphological aspects of all the samples. The GNS, CNT, and PANI/CNT/GNS materials were spectroscopically characterised after being prepared in powder form. A scanning electron microscope (SEM) is a type of electron microscope that scans a sample with a concentrated beam of electrons to produce pictures. Electrons interact with atoms in the sample, producing a variety of detectable signals that carry information on the surface topography and composition of the sample [58].

Figure 3.1 depicts SEM micrographs of pure PANI, PANI/CNT, and PANI/CNT/GNS nanocomposites with varying weight percentages of GNS loading. MWCNTs (CNT) are hollow cylindrical shaped tubes structure of carbon atoms, whereas graphene is two-dimensional sheets of carbon atoms. PANI displays surfaces that are rough, smooth, or flaky. According to (Fig. 3.1a-e), increasing the concentration of aniline monomer causes an increase in the degree of roughness and aggregation in the morphology of composites. The shape of the composite with the highest monomer concentration (Fig. 3.1b&c) revealed rough and heavily aggregated globules. This finding suggests that a higher monomer content in the initial polymerization solution resulted in a faster polymerization rate, resulting in a trough surface and poor adhesion. Because of this weak adherence, the contact resistance between the hybrid carbon assemblage substrate and PANI increases. The composite of PANI/CNT/3%GNS and PANI/CNT/5%GNS, on the other hand, lacks aggregated globular shape (Fig. 3.1d&e). This suggested that the polymer and three-dimensional hybrid carbon assemblage formed a strong bond.

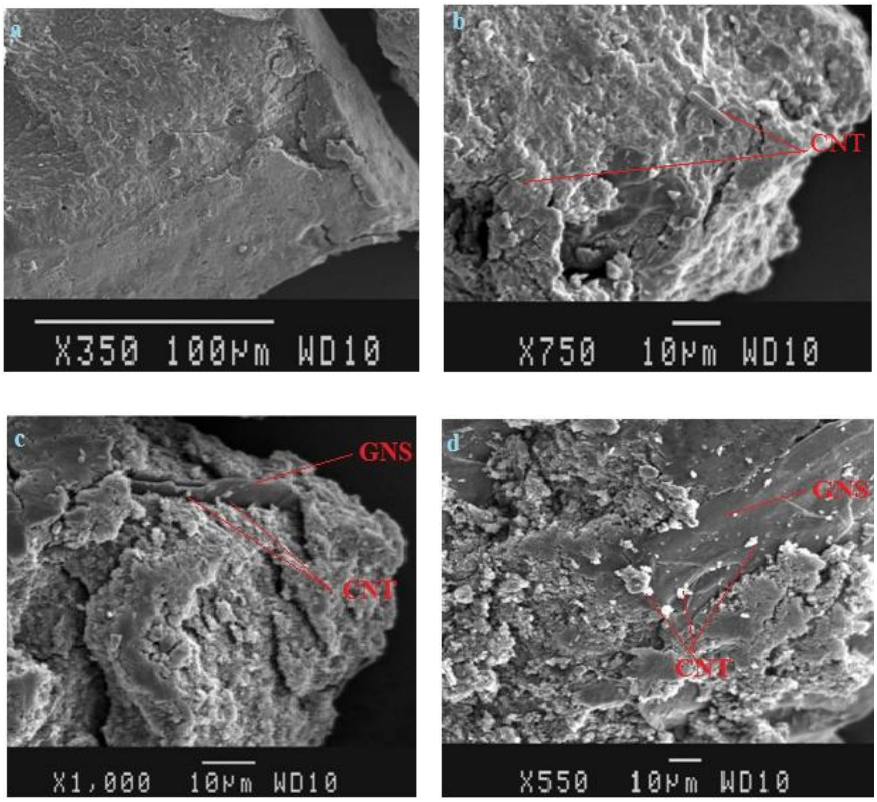

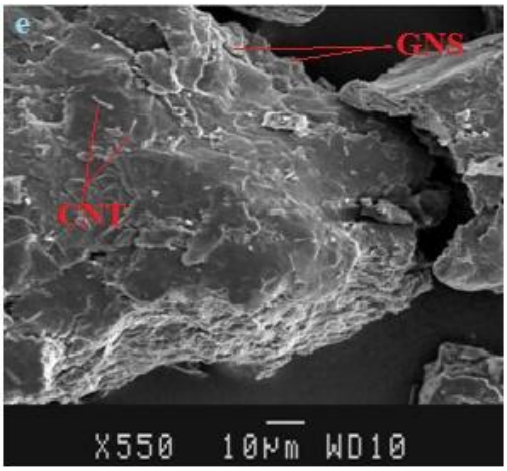

Figure 3.1: SEM Images (a)Pure PANI, (b)PANI/CNT, (c) PANI/CNT/1%GNS, (d) PANI/CNT/3%GNS, (e) PANI/CNT/5%GNS

MWCNTs are not independently visible in the PANI/CNT/3%GNS nanocomposite; there are places with a high concentration of agglomerated MWCNTs and small areas with an extremely negligible concentration of carbon nanotubes. Strong van der Waals interactions between carbon nanotubes could explain the agglomerates. Carbon nanotubes are sandwiched between PANI and graphene sheets. The interactions between the sheets of graphene nanoplatets result in huge agglomerates of GNS in PANI/CNT/5%GNS composites. A smooth GNS surface may result in weak interfacial interaction with the polymer. In the polymer matrix, GNS agglomerates of varied sizes are randomly distributed. The extent of visibility of the GNS rises as the GNS concentration in the nanocomposites grows, as do the nanotubes of various lengths seen and trapped in the polymer matrix. In addition, graphene sheets and MWCNTs can be seen in all of the samples [59,60].

B. Fourier Transform Infra Red:

The FT-IR spectroscopy identifies and confirms the structure and existence of various groups on the GNS sheet, as well as the presence of various linkages in PANI/CNT/GNS nanocomposites. This is a critical characterisation approach for chemical identification. The far infrared, or FIR, spectral spectrum spans 4000 to 500 cm-1 wavenumbers. This frequency range encompasses both backbone vibrations of big molecules and fundamental vibrations of molecules containing heavy atoms [61]. FT-IR has been frequently utilized to identify different types of chemical bonds (functional groups) in a molecule. FTIR spectroscopy is a technique for determining qualitative and quantitative properties of IR-active compounds in organic or inorganic solid, liquid, or gas samples. It is a quick and low-cost approach for analyzing crystalline, microcrystalline, amorphous, or film-like substances [62].

In the current study, the FTIR spectra of all materials were acquired using the KBr pellet technique on a Thermo Nicolet, Avatar 370 infrared spectrometer at Nagpur University's superior test and instrumentation laboratory.

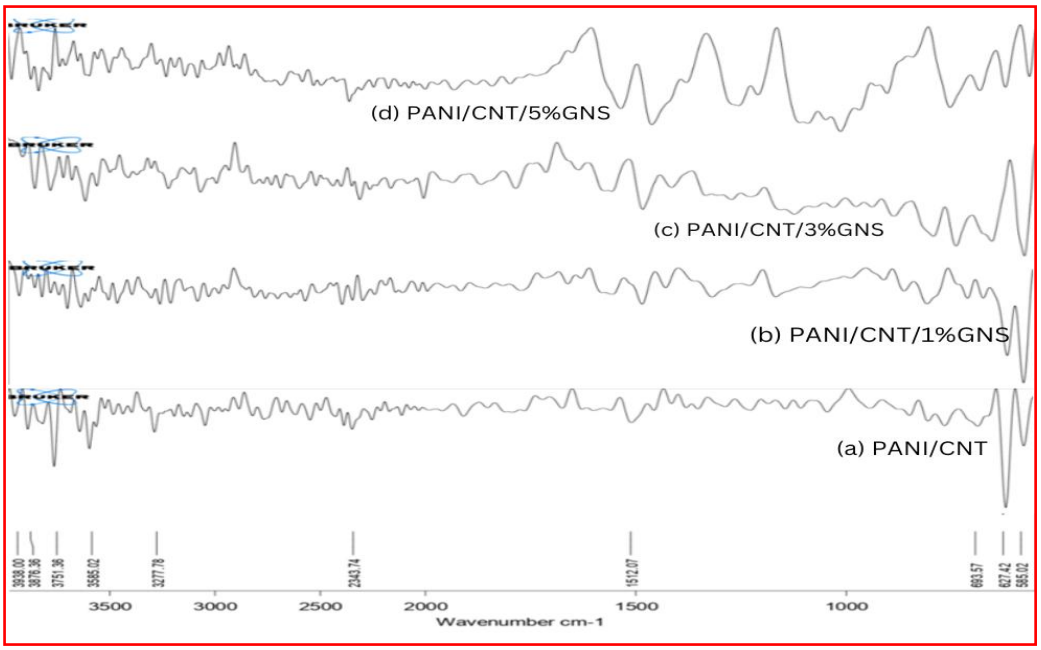

Figure 3.2: (a) PANI/CNT, (b) PANI/CNT/1%GNS, (c) PANI/CNT/3%GNS, (d) PANI /CNT/5%GNS

PANI/CNT FTIR spectra show peaks at 1512 cm^{-1} due to C=C bonds that create the framework of the CNT sidewall. However, after oxidation, certain new peaks are found in the composite that were not present in pure PANI, owing to MWCNT functionalization. The stretching mode of carboxylic groups connected to MWCNTs is associated with the peak at 1740 cm^{-1} [63]. The O-H stretching vibrations of carboxylic groups are responsible for the tiny peak at 3450 cm^{-1}. Acid functionalization is shown by these two peaks. These findings indicated that the MWCNTs were successfully oxidised into carboxylated carbon nanotubes. The absorption band at 1512 cm^{-1} is attributed to the MWCNT's skeletal vibration (Figure 3.2 a), which overlapped with the C=C stretching of PANI's quinone rings. The peaks at 1290 and 1105 cm^{-1} are attributed to the secondary aromatic amine group's C-N stretching vibration and aromatic C-H in plane bending vibration, respectively. The peak at 627 cm^{-1} corresponds to C-H out of plane bending vibration, and the minor peak at 693 cm^{-1} corresponds to para-distributed aromatic rings, indicating polymer production. The modest peak at roughly 1200 cm^{-1} is due to the conducting form of polyaniline, showing that it exists in conducting emaraldine form. This enables the creation of PANI on the MWCNT wall via an in-situ chemical polymerization process. Figure 3.2(b),(c),(d) depicts the FTIR spectra of PANI, hybrid carbon composite. The peak at 3479 cm-1 in the PANI hybrid carbon assemblage spectra corresponds to NH2 stretching, which changes to 3484 cm^{-1} with increased GNS concentration. The N-H bending of amine was represented by the peak at 1632 cm^{-1}. Furthermore, the peaks at 1176 and 1045 cm^{-1} are related to the primary structure of MWCNTs and graphene's C-C stretch vibration. The charge delocalization over the polymeric backbone is responsible for the modest peak about 1100 cm^{-1} (C-N stretching). NH_2 stretching vibrations caused the conspicuous peak at 3484 cm^{-1}. A minor shift in the position of the main characteristic peaks in the composite spectrum was found, indicating interaction of the hybrid carbon assemblage with PANI. This shows that the strong

interaction between PANI, MWCNTs, and GNS promotes an effective degree of electron delocalization, which improves polymer chain conductivity. The PANI linked to the hybrid carbon assemblage may be responsible for the rise in relative intensity of peaks around 3484, 1483, and 1045 cm^{-1} [64,65].

2. **Electrical Conductivity:** Filler content influences the electrical conductivity of polymer composites. The distance between conductive particles in an insulating polymer matrix with a low filler concentration is large, and conductivity is limited. Increased filler content in composites causes a non-linear increase in electrical conductivity as filler concentration increases. At a given filler concentration, known as the percolation threshold (c), the electrical conductivity of a composite quickly increases by several orders of magnitude, converting it from an insulator to a conductor. Sometimes a very small amount of conducting particles can be added to a filler to create an effective conducting channel, so making the entire composite conductive. CNTs and GNS could be used as effective fillers to build a conductive polymer composite with an extraordinarily low percolation threshold [66]. Percolation threshold values for MWCNT composites range from 0.002 to more than 2 wt.% [67-69] and from 1 to 8 wt.% for GNS composites [70, 71]. The importance of nanofiller content, aspect ratio, dimensions, and geometrical arrangement, as well as composite processing conditions, is demonstrated by such wide variances in percolation threshold values [72, 73]. The key challenges limiting polyaniline's expected improvement are that such nanoparticles create agglomerates due to vander Waals forces [74, 75], and a sufficient network in the polymer matrix is not generated, resulting in a higher percolation threshold. Agglomeration could be decreased by increasing the dispersion of the filler in the polymer matrix. Combining two carbon fillers into a hybrid structure is one of the most promising methods, which could result in a possibly new multifunctional material in research and application due to the synergy effect of both fillers, increasing mechanical, thermal, and electrical properties [76,77]. Smaller nanofillers with varying shapes provide a bigger surface area, allowing more polymer to come into touch with the filler. When the volume content of the nanofiller is high enough, the inter-phase becomes the dominant phase in the composite. Furthermore, the use of different forms of nanoparticles (1D - CNT and 2D - GNS) allows for increased efficiency at lower filler content. With the same number of filler particles and different geometrical arrangements of the chains, different particle lengths and shapes can be generated. In mixed MWCNT/GNS composites, electrical transport can occur via 1) electron hopping and tunneling in the MWCNT subsystem, 2) electron hopping and tunnelling in the GNS subsystem, and 3) electron tunneling between the GNS and MWCNT subsystems [78].

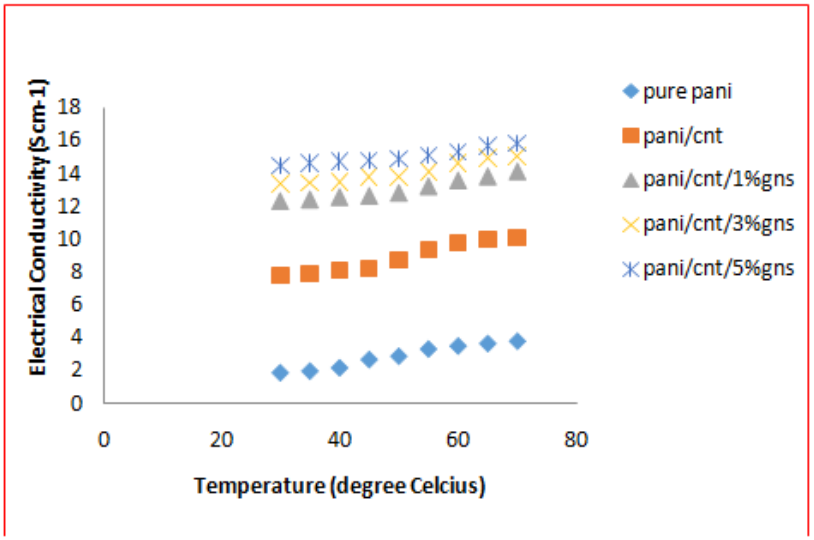

Figure 3.3: Variation of Electrical Conductivity with respect to temperature for PANI/CNT and different weight percent of GNS

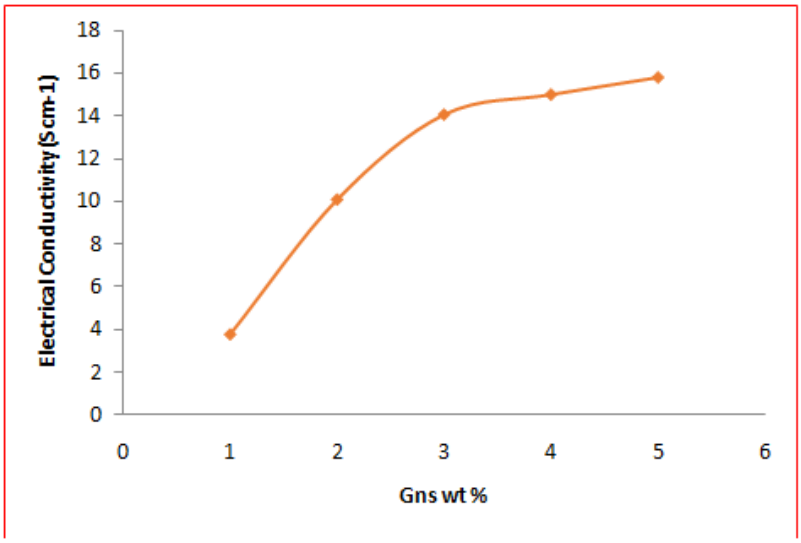

Figure 3.4: Variation of Electrical Conductivity with different weight percent of GNS in PANI/CNT

The increase in conductivity with increased GNS concentration for hybrid composites improved MWCNT distribution and electron tunneling between the GNS and the MWCNTs, resulting in an increase in electrical conductivity of mixed composites. The formation of a more effective conductive network as a result of the combination of MWCNT and GNS conductive particles could explain the increase in electrical conductivity of the conducting polymer [79].

An improved four probe electrical conductivity metre was used to measure the electrical conductivity of PANI/CNT/GNS nanocomposites with increasing GNS

concentration. The PANI class of conducting polymers is widely known; its electrical conductivity is in the order of 1-2 S cm_1 at ambient temperature, but it was found to be 3.8 S/cm at 80 degrees C. Graphene and MWCNTs have exceptionally high electrical conductivity when compared to PANI. However, the presence of multilayer graphene and MWCNTs has a considerable impact on the electrical conductivity of PANI. Previous research has shown that incorporating MWCNTs into PANI during processing boosts its electrical conductivity fourfold, which is linked to the formation of a conductive network. At room temperature, the electrical conductivity of nanocomposites was shown to be significantly higher than that of pure PANI. The electrical conductivity of the nanocomposite rises continually after reinforcing a varied weight percent of GNS in the PANI/CNT. The extent of increase in electrical conductivity, electrical conductivity is 10.11 S/cm for PANI/CNT and increases from 14.09, 15.03, 15.84 S/cm for PANI/CNT/1%GNS, PANI/CNT/3%GNS, PANI/CNT/5%GNS, respectively, as shown in figures 3.3 and 3.4. Because GNS has a high electrical conductivity, increased concentrations of GNS provide a good networking electrical conduction pathway. This is determined by the creation of a conductive network in the polymer matrix by MWCNTs and graphene.

3. **Electromagnetic Interferences Shielding Effectiveness:** The electromagnetic interference shielding performance of PANI/CNT nanocomposite material and hybrid assemblage or ternary nanocomposites of PANI/CNT/GNS was investigated. When compared to conventional materials, the polymer matrix incorporating nano particles of CNT and GNS improves the interfacial polarization and effective anisotropy energy of the sheets, resulting in higher scattering and high shielding effectiveness. The addition of nano particles such as CNT and GNS to PANI improves absorption properties, which are highly dependent on the volume fraction of the filler. As a result, absorption rather than reflection is responsible for the high value of EMI SE. The EMI shielding efficacy of all synthesized nanocomposites increases as the GNS concentration increases. The volume resistivity of composites decreases as GNS increases from 1% to 5%, whereas Shielding Effectiveness increases. The number of percolating networks grows as the number of GNS grows. Conductive networks produced by the dispersion of CNT and GNS act similarly to conductive meshes. As GNS loading increases, so does the size of the conductive mesh, which functions as a barrier to incident Electromagnetic radiations and results in greater EMI SE. This is due to the fact that the electrical conductivity of a composite tends to increase with increasing GNS content, and as a result of the action of electromagnetic radiation, induction current made on the interface or in the interior of the sample produces reversal electromagnetic field, which leads to an increase in surface reflection attenuation of electromagnetic wave, and thus the EMI shielding effectiveness of the composite increases. The attenuation of incident waves can be increased by increasing the absorption and scattering cross sections of absorbent particles. The incident wave energy is also attenuated more. The greater the specific surface area of GNS, the greater the plane wave absorption cross section and scattering cross section of the absorbing particle, and hence the greater the electromagnetic wave loss. The overall Shielding Effectiveness of PANI is widely known to be dominated by absorption phenomena caused by the presence of localised charges (polarons and bipolarons), resulting in a high divergence and relaxation impact. The PANI coating on the GNS can dominate the polarisation, and the functional groups of functionalized GNS and functionalized CNT result in electromagnetic radiation absorption. The functional groups

of GNS and CNT are also responsible for absorption; as the content of GNS grows, so do the functional groups responsible for electromagnetic radiation absorption. Many factors influence a material's EMI SE, including conductivity, dielectric constant, aspect ratio, state of dispersion of conductive fillers, and shielding material thickness. Conductivity is the most important factor for an EMI shielding material out of all of these. In the case of a conductive material such as metal, EMI SE is mostly caused by EM radiation reflection, whereas in the case of a conductive composite, EMI SE is primarily caused by radiation absorption.

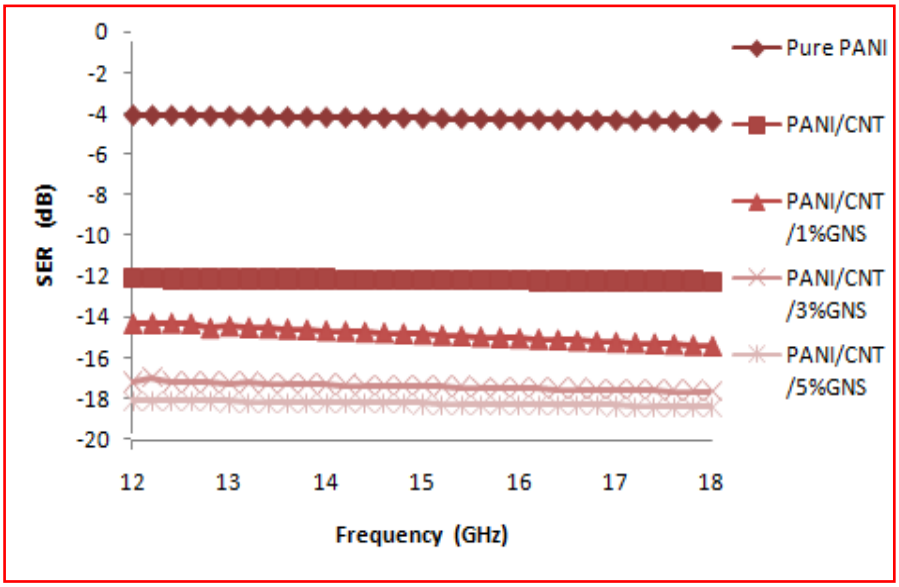

Figure 3.5: (a) Shielding Effectiveness due to Reflection

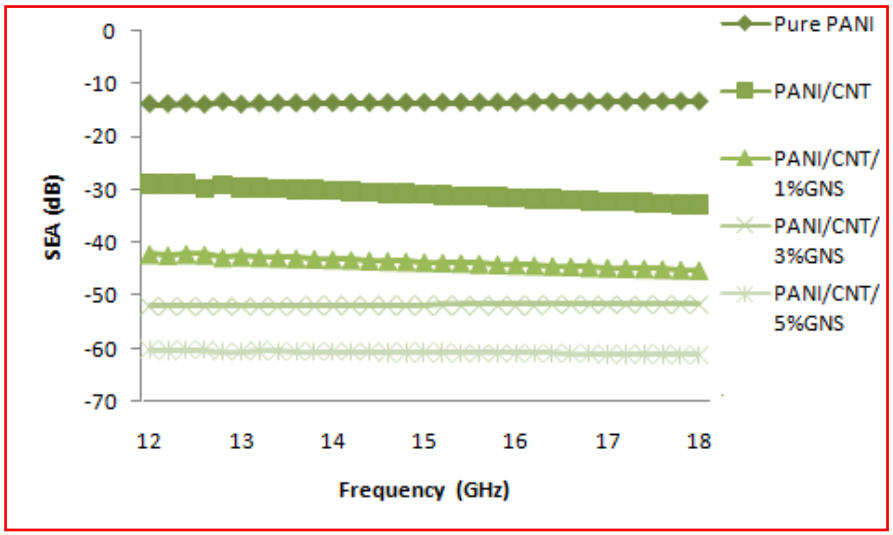

Figure 3.5: (b) Shielding Effectiveness due to Absorption

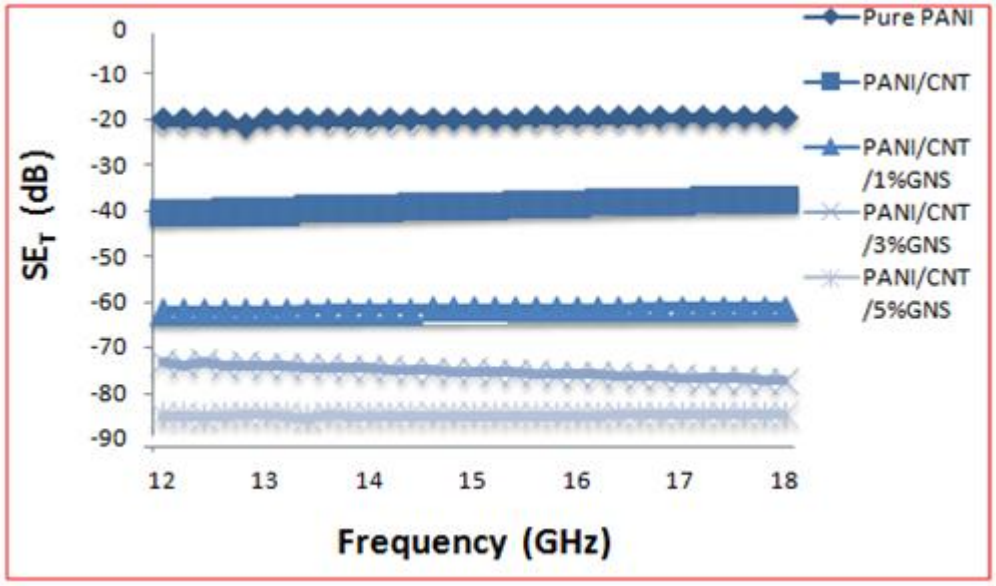

Figure 3.5: (c) Total Shielding Effectiveness of composites

Figure 3.5 (a), (b), and (c) show the SE_R, SE_A, and SE_T of PANI/CNT, and hybrid assemblage or ternary nanocomposites of PANI/CNT/GNS nanocomposites as a function of frequency in the range 12-18 GHz (Ku band) of weight% 1,3, and 5. The SE_R is almost linear for each composition across the whole frequency range of measurement and exhibits a small variation even as GNS loading increases. With a 1 to 3 wt% increase in GNS loading, the SE_A rises from 13 to 60 dB. According to the experimental data, absorption is the major shielding process, whereas reflection is the secondary shielding mechanism. The SE_T of nanocomposite as a function of frequency demonstrates that the nature of SE_T for each composition is almost linear with frequency, while the SE_T of composite is found to increase as GNS loading increases. The total electromagnetic interference shielding effectiveness of pure PANI, PANI/CNT, PANI/CNT/1%GNS, PANI/ CNT/3%GNS, and PANI/ CNT/5%GNS, respectively, is 20, 40, 61, 73, and 85 dB. The EMI SE of synthesized composites obtained is greater than the required EMI shielding efficacy (20 dB) for commercial applications. Such a high value of EMI SE with such a low loading of GNS demonstrates the outstanding efficiency. The EMI SE results reveal that synthesized composites have an absorption-dominant mechanism and can be employed to protect electronic equipment and components from electromagnetic radiation as lightweight, effective EMI shielding or microwave absorption materials.

IV. CONCLUSION

The PANI/CNT/GNS nanocomposites were synthesized in this study utilizing an in-situ chemical oxidation polymerization process with a modification in the weight fraction of GNS. SEM and FTIR were used to characterize the synthesized materials. The SEM pictures of PANI/CNT/GNS nanocomposites show that the GNS surface has been covered with a smooth thin polyaniline layer. Because of the contribution of PANI to the layered GNS surface, the surface is rough and the characteristic layered structure has vanished, revealing a coralline-like shape. There is no free GNS in PANI/GNS nanocomposites, indicating that the

PANI covers the GNS surface uniformly. Carbon nanotubes can also be found in the composites, but in modest amounts.

The vibration and rotation of the chemical bonding and molecular structures of the produced PANI/CNT/GNS nanocomposites are revealed by Fourier Transform Infrared Spectroscopy (FTIR).

The electrical conductivity of PANI/CNT/GNS composites was observed to increase as the weight percent of GNS in the PANI matrix increased. At room temperature, the electrical conductivity of nanocomposites was shown to be significantly higher than that of pure PANI.

The EMI shielding efficiency (SE) of PANI/CNT/GNS nanocomposites was studied in the 12-18 GHz frequency range using a vector network analyzer. EMI shielding involves three mechanisms: reflection, absorption, and multiple-reflection. Absorption is the major shielding mechanism for conducting polymer/hybrid carbon-based composites samples, followed by reflection shielding. The electromagnetic shielding effectiveness (SE) was found to increase with increasing GNS content. The obtained EMI SE for synthesized composites is greater than the required value of EMI shielding effectiveness (20 dB) for commercial applications. It was discovered that absorption was dominant, implying that PANI/CNT/GNS nanocomposites can be employed as lightweight EMI shielding materials.

REFERENCES

[1] Li-Li Wanga, Beng-Kang Tay, Kye-Yak See, Zhuo Sun, Lin-Kin Tan, Darren Lu, Electromagnetic interference shielding effectivenessof carbon-based materials prepared by screen printing, Carbon, (**2009**), 47,1905 –1910
[2] Lei Zhang, Research on preparation and property of alternating multilayer polymer electromagnetic shielding materials, Applied Mechanics and Materials, (**2014**), 443, 634-638
[3] Parveen Saini, Veena Choudhary, N. Vijayan, and R. K. Kotnala, Improved Electromagnetic Interference Shielding Response of Poly (aniline)-Coated Fabrics Containing Dielectric and Magnetic Nanoparticles, The Journal of Physical Chemistry, (**2012)**, 116 (24), 302131
[4] D.D.L. Chung, Electromagnetic interference shielding effectiveness of carbon Materials, Carbon, (**2001**), 39, 279–285
[5] Tassew Alemayehu, Biri Himariam, Synthesis and characterization of conducting polymers: a review paper, International Journal of Recent Research in Physics and Chemical Sciences, (**2014**), 1(1), 24-28.
[6] Khalil Arshak, Vijayalakshmi Velusamy, Olga Korostynska, Kamila Oliwa-Stasiak, and Catherine Adley, Conducting polymers and their applications to biosensors: emphasizing on foodborne pathogen detection, IEEE Sensors Journal, (**2009**), 9 (12), 1942-1951.
[7] Supri a. Ghani and Heah Chong Young, Conductive polymer based on polyaniline-eggshell powder (pani-esp) composites, Journal of Physical Science, (**2010**), 21(2), 81–97.
[8] A.K.Bakshi and Pooja Rattan, Electrically conducting polymers: An Emerging Technology, Current Science, (**1997**), 73(8), 648-651.
[9] En-Chung Chang, Mu-Yi Hua and Show-An Chen, Synthesis and properties of the water soluble self-acid-doped polypyrrole:poily[4-(3-pyrroleyl)butanesulfonic acid], Journal of Polymer Research, (**1998**), 5(4), 249-254.
[10] Manju Gerard , Asha Chaubey, B.D. Malhotra, Application of conducting polymers to biosensors, Biosensors & Bioelectronics , (**2002**), 17, 345–359.
[11] Song feng Pei, H ui-Ming Cheng, The reduction of graphene oxide, Carbon, (**2012**), 50, 3210 – 3228
[12] Ji gang Wang,Yong sheng Wangn, Da wei He n, Zhiyong Liu, Hongpeng Wu, Haiteng Wang, Pan Zhou,MingFu, Polymer bulk heterojunction photovoltaic devices based on complex donors and solution-processable functionalized graphene oxide, Solar Energy Materials & Solar Cells , (**2012**), 96, 58–65.

[13] Zhao yang Liu , Lei jing Liu , Hui Li , Qing feng Dong , ShiyuYao , Arnold B. KiddI V. , Xiao yu Zhang , Ji yang Li , Wen jing Tian , A ‘‘Green’’ polymer solar cell based on water-soluble poly [3-(potassium-6-hexanoate)thiophene-2,5-diyl] and aqueous-dispersible non covalent functionalized graphene sheets, Solar Energy Materials & Solar Cells, (**2012**), 97, 28–33

[14] Dale A.C. Brownson, Dimitrios K. Kampouris, Craig E. Banks, An overview of graphene in energy production and storage applications, Journal of Power Sources , (**2011**), 196, 4873–4885

[15] Ming-Yu Yen, Min-Chien Hsiao , Shu-Hang Liao , Po-I Liu , Han-Min Tsai, Chen-Chi M. Ma , Nen-Wen Pu, Ming-Der Ger ,Preparation of graphene/multi-walled carbon nanotube hybrid and its use as photoanodes of dye-sensitized solar cells. Carbon (**2011**), 49, 3597–3606

[16] Rong Kou, Yuyan Shao, Donghai Mei, Zimin Nie, Donghai Wang, z Chongmin Wang, Vilayanur V Viswanathan, Sehkyu Park, Ilhan A. Aksay, Yuehe Lin, Yong Wang, and Jun Liu, Stabilization of Electrocatalytic Metal Nanoparticles at Metal-Metal Oxide-Graphene Triple Junction Points, Chem. Soc. (**2011**), 133, 2541–2547

[17] Juha Riikonen , Wonjae Kim, Changfeng Li, Olli Svensk, Sanna Arpiainen, Markku Kainlauri, Harri Lipsanen, Photo-thermal chemical vapor deposition of graphene on copper, Carbon,(**2013**), 62,43– 50

[18] Tomo-o Terasawa , Koichiro Saiki , Growth of graphene on Cu by plasma enhanced chemical vapor deposition, Carbon ,(**2012**), 50, 869 –874

[19] Zhiyong Liu, Dawei He , Yongsheng Wang , Hongpeng Wu, Jigang Wang, Solution-processable functionalized graphene in donor/acceptor-type organic photovoltaiccells, Solar Energy Materials & Solar Cells , (**2010**),94, 1196–1200

[20] Douglas R. Kauffmanab and Alexander Star, Graphene versus carbon nanotubes for chemical sensor and fuel cell applications, The Royal Socity of Chemistry, (**2010**), 135, 2790–2797

[21] Reina, X. Jia, J. Ho, D. Nezich, H. Son, V. Bulovic, S. M. Dresselhaus and J. Kong, “Large Area, Few-Layer Graphene Films on Arbitrary Substrates by Chemical Vapour Deposition,” Nano Letters, (**2009**), 9, 1, 30-35

[22] D.W. Zhang, X.D. Li, H.B. Li, S. Chen, Z. Sun, X.J. Yin, S.M. Huang, Graphene-based counter electrode for dye-sensitized solar cells, Carbon, (**2011**), 49, 5382 –5388

[23] Mohammed Khenfouch1, U. Buttner, Mimouna Baïtoul, Malik Maaza. Synthesis and Characterization of Mass Produced High Quality Few Layered Graphene Sheets via a Chemical Method, Graphene, (**2014**), 3, 7-13

[24] Y.Y. Tan, K.D.G.I. Jayawardena, A.A.D.T. Adikaari, L.W. Tan, J.V. Anguita, S.J. Henley, V. Stolojan, J.D. Carey, S.R.P. Silva, Photo-thermal chemical vapor deposition growth of graphene. Carbon, (**2012**), 50, 668 –673

[25] Florentino López-Urías, Yadira I. Vega-Cantú, Fernando J. Rodríguez-Macías, Ana Laura Elías , Emilio Mu˜noz-Sandoval, Abraham G. Cano-Márquez, Jean-Christophe Charlier, Humberto Terrones , Graphene and graphite nanoribbons: Morphology, properties, synthesis, defects and applications. Nano Today, (**2010**), 5, 351-372

[26] Sumio Iijima, Carbon nanotubes: past, present, and future, Physica B 323 (**2002**) 1–5

[27] T. Belin, F. Epron, Characterization methods of carbon nanotubes: a review, Materials Science and Engineering B 119 (**2005)** 105–118

[28] Ray H. Baughman, Anvar A. Zakhidov, Walt A. de Heer, Carbon Nanotubes—the Route Toward Applications,science copass (**2022**)vol. 297 ,787-792

[29] Michael F. L. De Volder, Sameh H. Tawfick,4,5 Ray H. Baughman,6 A. John Har, Carbon Nanotubes: Present and Future,Commercial Applications,science compass (**2013)** vol 339 ,535-539

[30] Pulickel M. Ajayan1 and Otto Z. Zhou, Applications of Carbon Nanotubes, Appl. Phys. 80, 391–425 (**2001**)

[31] **William Gacitua E., Aldo Ballerini A. , Jinwen Zhang,** Polymer Nanocomposites: Synthetic and Natural Fillers- A Review, Maderas.Ciencia y tecnologia , (**2005**), 7(3),159-178

[32] Tapas Kuilla, Sambhu Bhadra, Dahu Yao, Nam Hoon Kim, Saswata Bose, Joong Hee Leea, Recent advances in graphene based polymer composites, Progress in Polymer Science, (**2010**), 35, 1350–1375

[33] Omar A. Al-Hartomy, Ahmed Al-Ghamdi, Nikolay Dishovsky, Rossitsa Shtarkova, Vladimir Iliev, Ibrahim Mutlay, Farid El-Tantawy, Dielectric and Microwave Properties of Natural Rubber Based Nanocomposites Containing Graphene, Materials Sciences and Applications, (**2012**), 3, 453-459

[34] K. Saravanan , S. Sathiyanarayanan, S. Muralidharan, S. Syed Azim, G. Venkatachari, Performance evaluation of polyaniline pigmented epoxy coating for corrosion protection of steel in concrete environment, Progress in Organic Coatings , (**2007**),59, 160–167

[35] Shiow-Jing Tang, An-Tsai Wang, Su-Yin Lin, Kuan-Yeh Huang, Chun-Chuen Yang, Jui-Ming Yeh and Kuan-Cheng Chiu, Polymerization of aniline under various concentrations of APS and HCl, Polymer Journal, (**2011**), 43, 667–675
[36] Sunil K. Pillalamarri, Frank D. Blum, Akira T. Tokuhiro and Massimo F. Bertino, One-Pot Synthesis of Polyaniline-Metal Nanocomposites ,Chem. Mater., (**2005**), 17, 5941-5944
[37] Tian Chen, Jinhao Qui, Kongjun Zhu, Yincheng Che,Yunn Zhang, Jiamin Zhang, Hao Li, Fei Wang, Zhenzhen Wang, Enhanced electromagnetic wave absorpyion properties of polyanilline-coated Fe3O4/reduced graphene oxide nanocomposites, J Mater Sci. Mater Electron,(**2014**), 25,3661-3673
[38] Hua Bai,Yuxi Xu , Lu Zhao ,Chun Li and Gaoquan Shi . Non-covalent functionalization of graphene sheets by sulfonated polyaniline, Chemical Communication (**2009**), 1667-1669
[39] Mohamad Fahrul Rajdi Hanifah, Juhana Jaarfar, Madzlan Aziz, A. F. Ismail, M H D Othman and Mukhlis A Rahman, Effect of reduction time on the structural, electrical and thermal properties of synthesized reduced graphene oxide nanosheets, Bull. Mater Sci. (2015), 38, 6, 1569-1576
[40] Deepak Kumar, Anjan Banerjee, Satish Patil and Ashok Shukla, A 1V Supercapacitor device with nanostructured graphene oxide/polyaniline composite materials, Bull. Mater Sci.(**2015**), 38(6), 1507-1517
[41] Qingli Hao, Hualan Wang, Xujli Yang, Lude Lu and Xin Wang, Morphology- controlled fabrication of sulphonated Graphene/Polyaniline Nanocomposites by Liquid/Liquid Interfacial Polymerization and Investigation of their Electrochemical Properties, Nano Res, (**2011**),4(4),323-333
[42] Avanish Pratap Singh, Parveen Garg, Firoz Alam, Kuldeep Singh, R.B.Mathur, R.P,Tandon, Amita Chandra, S.K.Dhawan, Phenolic resin-based composite sheets filled with mixtures of reduced grapheneoxide, ϒ-Fe2O3 and carbon fibers for excellent electromagnetic interference shielding in the X-band, Carbon,(**2012**), 50, 3868-3875
[43] Mei Li, Yunqiang Zhang, Lanlan Yung, Yingkai Liu, Jingyun Ma, Excellent electrochemical performance of homogenous polypyrrole/graphene composites as electrode material for supercapacitors , Journal of Materials Science: Materials in Electronics, (**2015**), 26_1, 485-492
[44] Y. S. Lim, Y.P. Tan, H.N.Lim, N.M.Huang, W.T. Tan, Preperation and charecterization of polypyrrole/graphene nanocomposite films and their electrochemical performance,J. Polym Res, (**2013**), 20,156-163
[45] Saswata Bose, Nam Hoon Kim, Tapas Kuila, Kin-tak Lau,Electrochemical performance of a graphene-polypyrrole nanocomposite as a supercapacitor electrode,Nanotechnology, (**2011**), 22, 295202-295213
[46] Saswata Bose, Ananta Mishra, Partha Khanra, Nam Hoon Kim, Joong Hee Lee ، Chemical functionalization of graphene and its applications, Progress in Materials Science,(**2012**), 57(7), 1061–1105
[47] Hannes C. Schniepp , Je-Luen Li , Michael J. McAllister , Hiroaki Sai , Margarita Herrera-Alonso , Douglas H. Adamson , Robert K. Prud'homme , Roberto Car , Dudley A. Saville , and Ilhan A. Aksay, Functionalized Single Graphene Sheets Derived from Splitting Graphite Oxide, *J. Phys. Chem. B*, (**2006)**, *110* (17), 8535–8539
[48] Nicolas A. Cordero and Julio A Alonso, The interaction of sulphuric acid with graphene and formation of adsorbed crystals, Nanotechnology, (**2007**), 18(48), 485705
[49] Claudia Bautista-Flores, Roberto Ysacc Sato-Berrú, D. Mendoza1, Doping Graphene by Chemical Treatments Using Acid and Basic Substances, Journal of Materials Science and Chemical Engineering, (**2015**), 3, 17-21
[50] Ngo Trinh Tung, Tran Van Khai, Minhee Jeon, Yeo Jin Lee, Hoeil Chung, Jeong-Hwan Bang and Daewon Sohu, Preperation and Charecterization of nanocomposite based on Polyaniline and Graphene nanosheets, Macromolecular Research, (**2011)**, 19(2),203-208
[51] Guangmin Zhou, Dawei Wang, Hui-ming Cheng, Feng Li, Synthesis and electrochemical properties of Pani/Carbon nanostructure composite,(**2010**),1-2
[52] C. Harish, V. Sai SreeHarsha, C. Santhosh, R. Ramachandran, M. Saranya, T. Mudaliar Synthesis of Polyaniline/Graphene Nanocomposites and Its Optical, Electrical and Electrochemical Properties, Advanced Science, Engineering and Medicine, (**2012**), 4, 1–9,
[53] Vanchinathan, K. Govardhan, and A. Nirmala Grace Wen Ling Zhang and Hyoung Jin Choi, Dynamic Response of a grapheme Oxide- Polyaniline Composite Suspension
[54] Sachin B. Kulkarni, Umakant M. Patil, Iman Shsckery,Ji Soo Soo Sohn, Suchan Lee, Byeongho Park and SeongChan Jun, High performance supercapacitor electrode based on a polyaniline nanofibers/3D grapheme framework as an efficient charge transporter ,J Matar Chem A, (**2014**) ,2, 4989-4998
[55] Xinlu Li, Engfang Song, Yonglai Zhang, Hao Wang, Kun Du, Hongvi Li, Yuan Yuan, Jiamu Huang, Enhanced Electrochemical Capacitance of Graphene Nanosheets coating with Polyaniline for Supercapacitors, Int. J. Elecochem. Sci.,(**2012**), 7, 5163-5171

[56] Jieum Kim, Soo-Jin Park and Seok Kim, Capacitance behaviours of Polyaniline/Graphene nanosheet Composites Prepared by Aniline Chemical Polymerization, Carbon Letters ,(**2013**), 41(1),51-54
[57] Zhou Guang Min, Wang Da-Wei, Li Feng, Zhang Li-li, Weng Zhe, Chang Hui Ming, The effect of carbon particle morphology on the electrochemical properties of nanocarbon/ polyaniline composites in supercapacitors, New Carbon Materials,(**2011**), 26(3), 0180-0186
[58] S. Mukhopadhyay, Sample Preparation for Microscopic and Spectroscopic Characterization of Solid Surfaces and Films: Sample Preparation Techniques in Analytical Chemistry, John Wiley & Sons, Inc. (**2003**), 377-411.
[59] I. Kranauskaitė, J. Macutkevič, A. Borisova, A. Martone, M. Zarrelli, A. Selskis , A. Aniskevich, and J. Banys, enhancing electrical conductivity of multi walled carbon nanotube/epoxy composites by gra phene nano platelet s**,** Lithuanian Journal of Physics, 57, (**2017**),4, 232–242
[60] Pashupati Pokharel , Dequan Xiao , Folarin Erogbogbo , Ozgur Keles b, Dai Soo Lee, Electrically conductive network structure in polyurethane nanocomposites using a hybrid of graphene nanoplatelets,carbon black and multi-walled carbon nanotubes , Composites Part B: Engineering, 161, (2019), 169-182
[61] S. Pareek, K. Pareek, An Empirical Study on Structural, Optical and Electronic Properties of ZnO Nanoparticles, IOSR-Journal of Applied Physics (**2013**), 3, 16-24.
[62] P.L. King, M.S. Ramsey, P.F. McMillan & G. Swayze, Laboratory Fourier Transform Infrared Spectroscopy Methods for Geologic Samples**, Molecules to Plants: Infrared Spectroscopy in Geochemistry, Exploration Geochemistry and Remote Sensing,(2004),** 5, 57-92
[63] S. G. Bachhav, D. R. Patil, Synthesis and Characterization of Polyaniline-Multiwalled Carbon Nanotube Nanocomposites and Its Electrical Percolation Behavior, American Journal of Materials Science (**2015**), 5(4): 90-95
[64] Ashok K. Sharma, Preetam Bhardwaj, Kamal Kant Singh &Sundeep K. Dhawan, Improved microwave shielding properties of polyaniline grown over three-dimensional hybrid carbon assemblage substrate, Appl Nanosci (**2015**) 5:635–644.
[65] Tejendra K. Gupta, Bhanu Pratap Singh, Rakesh B. Mathur and Sanjay R. Dhakate, Multi-walled carbon nanotube–graphene–polyaniline multiphase nanocomposite with superior electromagnetic shielding effectiveness, Nanoscale, (2014), 6, 842–851
[66] J.N. Coleman, U. Khan, W.J. Blau, and Y.K. Gun'ko,Small but strong: A review of the mechanical properties of carbon nanotube–polymer composites, Carbon 44(9), 1624–1652 (**2006**).
[67] J.K.W. Sandler, J.E. Kirk, I.A. Kinloch, M.S.P. Shaffer, and A.H. Windle, Ultra-low electrical percolation threshold in carbon-nanotube-epoxy composites, Polymer 44(19), 5893–5899 (**2003**).
[68] C.A. Martin, J.K.W. Sandler, M.S.P. Shaffer, M.K. Schwarz, W. Bauhofer, K. Schulte, and A.H. Windle, Formation of percolating networks in multi-wall carbon-nanotube-epoxy composites, Compos. Sci. Tech. 64(15), 2309–2316 (**2004**).
[69] S.Y. Fu, X.Q. Feng, B. Lauke, and Y.W. Mai, Effects of particle size, article/matrix interface adhesion and particle loading on mechanical properties of particulate–polymer composites, Compos. B Eng. 39(6), 933–961 (**2008**).
[70] J.B. Bai and A. Allaoui, Effect of the length and the aggregate size of MWNTs on the improvement efficiency of the mechanical and electricalproperties of nanocomposites – experimental investigation, Composites A 34(8), 689–694 (**2003**).
[71] X.M. Chen, J.W. Shen, and W.Y. Huang, Novel electrically conductive polypropylene/graphite nanocomposites, J. Mater. Sci. Lett. 21(3), 213–214 (**2002**).
[72] W.G. Weng, G.H. Chen, D.J. Wu, and W.L. Yan, HDPE/expanded graphite electrically conducting composite, Compos. Interface 11(2), 131–143 (**2004**).
[73] I. Neitzel, V. Mochalin, and Y. Gogotsi, Ultrananocrystalline. Diamond (Elsevier, **2012**).
[74] T. Glaskova, M. Zarrelli, A. Borisova, K. Timchenko, Aniskevich, and M. Giordano, Method of quantitative analysis of filler dispersion degree in composite systems with spherical inclusions, Compos. Sci. Technol. 71(13), 1543–1549 (**2011**).
[75] A.S. Patole, S.P. Patole, S.Y. Jung, J.B. Yoo, J.H. An, and T.H. Kim, Self assembled graphene/carbon nanotube/polystyrene hybrid nanocomposite by *in situ* microemulsion polymerization, Eur. Polym. J. 48(2), 252–259 (**2012**).
[76] U. Khan, I. O'Connor, Y.K. Gun'ko, and J.N. Coleman, The preparation of hybrid films of carbon anotubes and nano-graphite/graphene with excellent mechanical and electrical properties, Carbon 48(10), 2825–2830 (**2010**).

[77] S. Chatterjee, F. Nafezarefi, N.H. Tai, L. Schlagenhauf, F.A. Nuesch, and B.T.T. Chu, Size and synergy effects of nanofiller hybrids including graphene nanoplatelets and carbon nanotubes in mechanical properties of epoxy composites, Carbon 50(15), 5380–5386 (**2012**).
[78] Balberg, Tunnelling and percolation in lattices and the continuum, J. Phys. D 42(6), 064003 (**2009)**.
[79] Kranauskaitė, J. Macutkevič, A. Borisova, A. Martone, M. Zarrelli, A. Selskis. Aniskevich, and J. Banys, Enhancing electrical conductivity of multiwalled carbon nanotu be/epoxy composites by grapheme nano platelets, Lithuanian Journal of Physics, Vol. 57, No. 4, pp. 232–242 (**2017**)

